Study of the Influence of IPPD on Thermo-Oxidation Process of Elastomeric Hose

X. Colom, F. Andreu-Mateu, F. J. Cañavate, R. Mujal, F. Carrillo

Chemical Engineering Department, EUETIT-UPC, Colom 1, Terrassa 08222, Spain

ABSTRACT: The aim of this study was to determine the influence of the *N*-isopropyl-*N'*-phenyl-*p*-phenylenediamine (IPPD) antioxidant agent on degradation of composites NBR/SiO$_2$. The inhibition of the early stages of the degrading process has been particularly analyzed.

Several NBR-SiO$_2$ matrix samples with and without IPPD have been exposed to an oxidizing atmosphere at 140°C for periods between 0 and 120 h. Besides, IPPD alone has been subject to the same aging thermo-oxidizing process. The degraded samples have been characterized by ATR-FTIR, TG, and SEM. Mechanical properties and degree of crosslinking have been determined. The results show that the IPPD improves the mechanical behavior of the composites submitted to thermo-oxidization, increasing the time in which composite retains rather good mechanical properties. IPPD decreases the ability of crosslinking of the rubber. ATR-FTIR spectroscopy study shows that the degradation process increases the volatility of the plasticizer and generates new unsaturation sites, which later will be the nuclei of crosslinking. © 2009 Wiley Periodicals, Inc. J Appl Polym Sci 114: 2011–2018, 2009

Key words: thermo-oxidation; NBR; SiO$_2$; IPPD

INTRODUCTION

Elastomeric materials have specific characteristics that make them useful for many chemical handling applications. Elastomeric hoses are included in most common pipe systems. Among other rubbers, nitrile butadiene is used in chemical engineering applications because of its combination of excellent resistance to oil or aromatic hydrocarbons and good elongation properties. On the other hand, Nitrile Butadiene rubber has limited weathering resistance and is affected by high temperatures. When exposed to a thermo-oxidizing atmosphere, substantial changes in mechanical properties are observed. Thermo-oxidizing aging promotes the crosslinking of rubbers and thermoplastics.[1–4] The aging process also results in chain degradation. Autocatalytic reactions between free radicals from unsaturated NBR with oxygen lead to oxygen containing functional groups as ketone, acid, aldehyde, alcohol, and epoxy. Antioxidant IPPD is added to prevent these undesirable effects, minimize aging and increase polymer lifetime. The protection mechanism and kinetics are known partially and still in study.[5,6] FTIR spectroscopy has proved to be a useful tool to advance in the knowledge of chemical behavior of IPPD[7] and analog compounds as *N*-phenyl-*N'*-(α-methylbenzyl)-*p*-phenylenediamine (SPPD).[8] The group of *p*-phenylenediamines antioxidants are the most important group of antioxidants used in rubber industry. Comparative studies of several derivatives have been performed to determine effectiveness and other characteristics.[9] Study of para-substituted anilines as model structures of amine-type antioxidant are also available.[10]

It is widely accepted that thermo-oxidation of NBR occurs in four stages: induction period, fast oxidation, slow oxidation and forbidden diffusion.[11,12] Because of the unsaturations present in the NBR, thermo-oxidizing process produces crosslinking developed initially on the surface. The surface becomes coated by a crosslinked layer that acts slowing down the degradation process.[13] This phenomenon can be studied by means of FTIR-ATR, SEM, TG, and by monitoring the degree of crosslinking of the sample.

In this work, an NBR elastomer of high content in butadiene (BD), including a large amount of fine silica and other additives was exposed to a thermo-oxidizing atmosphere. The effect of IPPD antioxidant agent on the chemical structure and mechanical properties of the composite during the aging process was studied.

MATERIALS AND METHODS

Samples preparation

NBR elastomeric blends were prepared in two steps: mixing and vulcanization. NBR (acrylonitrilebutadiene rubber) supplied by Lanxess GmbH, with less than 20% in acrylonitrile was used. The initial blends were prepared by adding 32 pphr of fine silica (135 m^2/g) and 28 pphr of dioctyl phtalate (DOP) to NBR previously softened in a two roll mixer (Collin type W 110E/P model). Then, 5 pphr of ZnO, 1.5 pphr of diphenylguanidine (DPG), 1.5 pphr of disulphur of 2-benzothiazole (MBTS), 0.25 pphr of Rhenogram Hexa, 1.8 pphr of sulfur, and 4 pphr of IPPD were added and homogenized. Components were mixed at 60°C of temperature controlling the adding sequence of the components and the optimal distance in the gap of the rolls.

Silica improves stability during the vulcanization and high temperature. Its slight polar character provides good dispersibility in the elastomer. ZnO accelerates the vulcanization and increases the strength. DOP is a compatible softener that provides flexibility. DPG accelerates the vulcanization, usually in combination with thiazoles. It also has good dispersibility in rubber. MBTS accelerates the vulcanization in combination with ZnO and sulfur, but it requires the presence of alkaline guanidine. Rhenogram Hexa and sulfur are vulcanizers. All chemicals were used as received from General Quimica SA (Spain).

The vulcanization was carried out in a hot (150 × 150 × 2 mm) plates square press (Collin mod. P200E) at 170°C for 15 min and 1.96 MPa of pressure. The cooling process was carried out under pressure and using cool water for refrigeration for 5 min. Test samples were properly shaped according to ISO 37:1994.[14]

Thermo-oxidizing process

The aging treatment was performed in an air-forced oven at 140°C. Samples were exposed for different time periods (0–120 h) according to ISO 4577.[15]

Thermal characterization

Thermal characterization was performed by means of thermogravimetric analysis (TGA) performed in a TGA851 Mettler Toledo unit. The elastomeric samples were cut into pieces about 3 mg. The TG thermograms were generally obtained in the temperature range of 50 to 600°C at a heating rate of 10°C min^{-1}. The experiments were carried out in air atmosphere to replicate real working conditions.

FTIR analysis

The spectra were acquired by using an Avatar 320 from Nicolet spectrometer equipped with a CsI optical collimated and a Horizontal Attenuated Total Reflectance (HATR) accessory. The internal reflecting element (IRE) was a ZnSe crystal set at an incidence angle of 45°. ATR-FTIR spectra were collected in the range of 4000 – 650 cm^{-1} with 40 scans and a resolution of 4 cm^{-1}.

Mechanical properties and hardness

Tensile tests were carried out following the specifications of the ASTM-D-412-98 to determine the evolution of Young's modulus, toughness, tensile strength, and the percentage of breaking deformation. A standard tension testing system Instron 3300 series was used. Displacement rate was 10 mm/min. The apparatus was fitted with an HRD automatic extensometer. Measurements were taken at a temperature of 23 ± 2°C and at a relative humidity of 50 ± 5%. Toughness of samples was calculated from measurements of the area of strength–strain curves.

Hardness was measured on a Shore D apparatus. Initial and after 60 s values were acquired.

Scanning electron microscopy

The fracture surface of the samples from mechanical testing was examined with a JEOL JSM 6480 scanning electron microscope. Dry samples were coated with a thin layer of carbon before observation under the microscope, to increase the sample conductivity.

Degree of crosslinking

A test piece of about 0.5 g was cut from the NBR plate. The sample was immersed in pure toluene at room temperature for 2 days to allow the swelling to reach diffusion equilibrium. Finally, the piece was removed and the adhered toluene was removed with filter paper. The crosslinking density was calculated using the Flory-Rehner equation.[16]

$$M_x = -(v_1 \rho_2)(v_2^{1/3})/[\ln(1 - v_2) + v_2 + \chi_1 v_2{}^2)]$$

where M_x is the M_W average between knots, v_1 is the toluene's molar volume; v_2 is the volume fraction of NBR in the swollen network in equilibrium with pure solvent, which was calculated using the Ellis and Welding equation[17]; ρ_2 is the density of the composite of NBR when it is not swollen; and χ_1 is the polymer–solvent interaction parameter calculated using Hildebrandt's equation[18]:
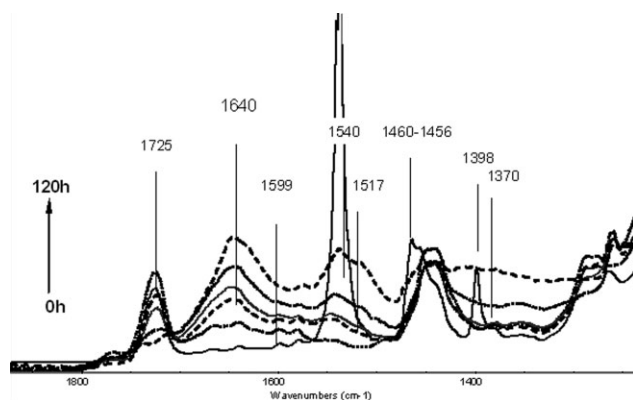
Figure 1 ATR-FTIR spectra in the area 1800 to 1300 cm^{-1} of NBR thermooxidated from 0 to 120 h (0, 12, 24, 48, 84, and 120 h).

$$\chi = \beta v_1 / RT(\delta_1 - \delta_2)$$

where β is the lattice constant, which was taken to be 0.34; R is the universal gas constant; T is the absolute temperature; and $\delta 1$ and $\delta 2$ are the solubility parameters of the solvent and the polymer respectively. The final value of χ calculated using this method for the NBR-toluene system was $\chi = 0.34/T$ (K).

RESULTS AND DISCUSSION

Spectral FTIR-ATR characterization and comparison between NBR with and without IPPD as antioxidant

Samples of elastomer with and without IPPD were submitted to the thermo-oxidizing conditions. Chemical changes were studied by ATR-FTIR spectroscopy. Figures 1 and 2 show the ATR-FTIR spectra obtained for the elastomeric materials (with and without IPPD) for a period of thermodegradation
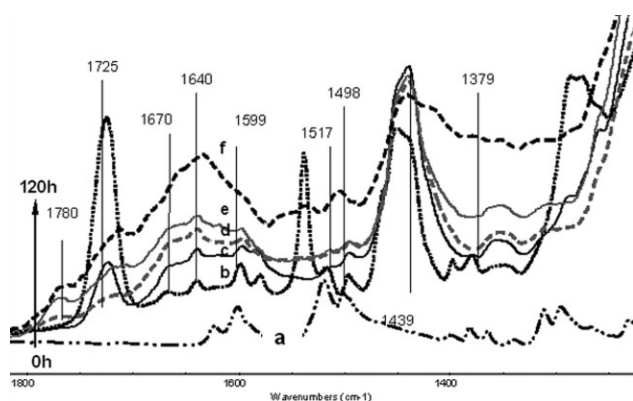

Figure 2 ATR-FTIR spectra in the area 1800 to 1300 cm^{-1} of IPPD and NBR$_{IPPD}$ thermooxidated from 0 to 120 h a, IPPD; b, NBR$_{IPPD}$ 0 h; c, NBR$_{IPPD}$ 24 h; d, NBR$_{IPPD}$, 48 h; e, NBR$_{IPPD}$ 84 h; f, NBR$_{IPPD}$ 120 h.

TABLE I
ATR-FTIR Characteristic Bands of the NBR Samples

Band (cm^{-1})	Assignation	Component
1379	C—H bend symmetric, methyl group iso	IPPD
1398	Zn carboxylic salts	ZnO
1460	C—H methylene	DOP
1498	C—H mono-substituted benzene	IPPD/IPQDI
1517	C—H para-substituted benzene	IPPD
1540	Zn carboxylic salts	ZnO
1599	C—H mono-substituted benzene	IPPD/IPQDI
1640	—CH=CH—	PBD
1670	>C=N—H stretch	Imino
1725	Oxygen containing struct. mainly =CO	DOP

from 0 to 120 h. Table I shows the main ATR-FTIR bands of the NBR samples analyzed.[19–21]

The analysis of the spectra showed the surface changes associated with the thermo-oxidation originated by the exposure of the elastomers to the degradation process. Figure 1 shows the evolution of NBR without IPPD. The band related to carbonyl group (1725 cm^{-1}) increases during the first step of the thermo-oxidation, but after approximately 12 h, it starts decreasing slowly. This behavior could be explained by the initial thermal shock that promotes the formation of carbonyl groups of ketone and aldehyde generated from the oxidation.[5] After this initial period (12 h), there is a disappearance of carboxylic groups from the surface. The decreasing in the carbonyl groups can be associated with the volatilization of DOP described by Mrklic and Kovacic.[22] There is a migration of DOP toward the surface that ends in volatilization. As a result of this process, the content of DOP in the core of the sample decreases. This phenomenon agrees with the quick decrease in methylene groups of the DOP plasticizer (shoulder at 1460 cm^{-1}), and is related to the elasticity decrease observed in mechanical properties. Also, a fast extinction of the bands at 1540 and 1398 cm^{-1} assigned at ZnO can be observed. Delor et al.[23] observed the formation of Zn carboxylates during the vulcanizing process of polychloroprene, in the presence of organic acids. Bands at values close to 1540 and 1398 cm^{-1} have been associated with Zn carboxylates in the previous studies.[23–25] According to these considerations, the simultaneous decrease in ZnO and DOP could be related to a formation of volatile Zn carboxylates.

Figure 2 shows the evolution of the bands corresponding to IPPD and to NBR$_{IPPD}$ from 0 h to NBR$_{IPPD}$ 120 h. The bands at 1498 and 1599 cm^{-1}, both related to mono-substituted benzene rings, and the 1517 cm^{-1} band from para-substituted benzene
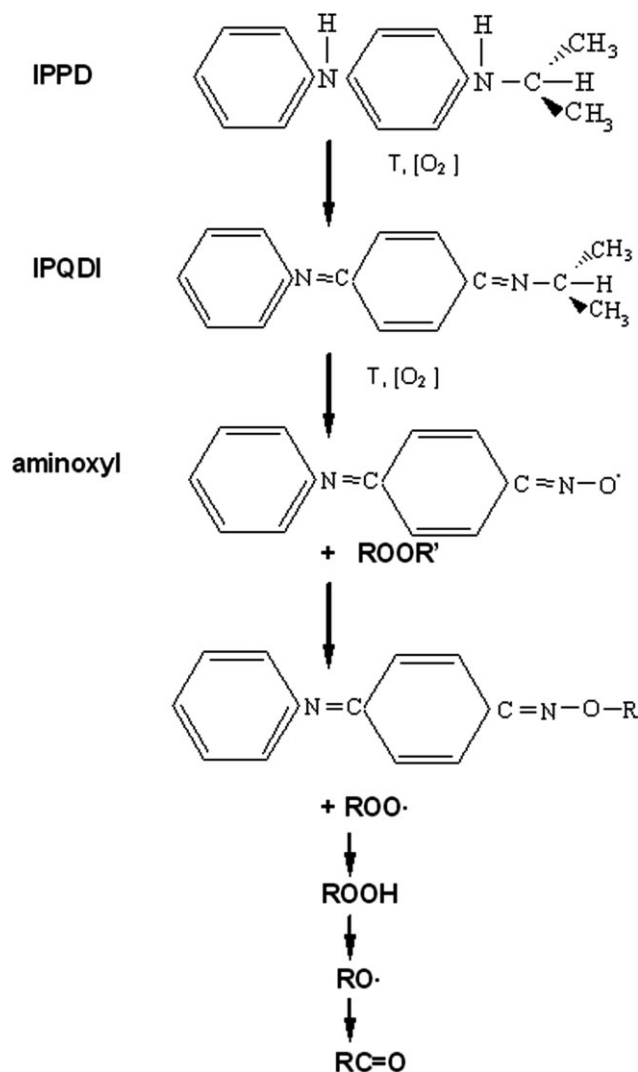
Figure 3 Thermal decomposition mechanism of IPPD with NBR at 140°C in oven.

rings,[19–21]characterize the benzene present in IPPD. There is a decrease in the para-substituted benzene band (1517 cm^{-1}) compared to the degraded mono-substituted IPPD band (1498 cm^{-1}) consequence of the degradation process. The peak at 1599 cm^{-1} decreases slowly in relation to the other two bands because it is related to N-isopropyl-N-phenyl quinone dimine (IPQDI), component generated in the degradation process of IPPD (Fig. 3).[6] Figure 2 shows that after 48 h (spectra d) there is still a perceptible amount of IPPD and its thermo-oxidation byproducts (bands at 1498 and 1599 cm^{-1}). Moreover, at 120 h all species generated from IPPD have nearly disappeared. This behavior agrees with the elastic and mechanical properties of the thermo-oxidized elastomer that will be discussed later.

A decrease in IPPD iso methyl group (1379 cm^{-1}) was observed. However, this change was not noticeable for short-time treatment, indicating that during the first stages of thermo-oxidation process, iso-methyl group disappears at the same rate as new ones are produced through radical reactions.[6] This result is related to the rather good properties observed in behavior the composites containing IPPD exposed at shorts periods of degradation.

The evolution of the NBR with IPPD is slightly different than the evolution of NBR without IPPD. The volatilization of the superficial DOP in the form of metallic esters is lower in samples of NBR$_{IPPD}$ (20 h) than in NBR without antioxidant (12 h).[5] During the first period of the degradation process (until 84 h), the band related to unsaturations (1640 cm^{-1}) observed in NBR$_{IPPD}$ is smaller than in the samples without IPPD, because the radicals generated in the process end their activity by reaction with the antioxidant. When the time of degradation increases, the band at 1640 increases significantly as shown in Figure 2. Moreover, a band that appears at 1670 cm^{-1} assigned to imino group (IPQDI) and a band at 1780 cm^{-1}, due to the formation of carbonyl compound (different from the DOP) by means of the reaction of aminoxyl radical with peroxide radicals formed during the degradation process of NBR. This mechanism is shown in Figure 3.[23,26]

Mechanical properties

The mechanical properties of NBR samples, with and without IPPD, are shown in Figures 4–8. The presence of IPPD in nonexposed NBR results in a slight increase in some mechanical properties, especially tensile strength. This increase may be explained by the plasticizer effect of the antioxidant and by its stabilizing effect avoiding degradation during the preparation of the samples. Overall, the elastic behavior of both types of NBR shows similar trends. Thermo-oxidation promotes structural changes by the chemical mechanisms discussed previously (section 3.1) producing a decrease in elongation and increase in Young's modulus. Toughness and tensile strength decrease with the exposure time. However, the presence of IPPD delays the loss of elasticity produced by thermo-oxidization. The addition of the antioxidant avoids partially the fast volatilization of DOP and the generation of unsaturations that cause rubber crosslinking. For this reason, at short times of thermo-oxidation, the NBR$_{IPPD}$ shows higher tensile strength, elongation and toughness. However, after 48 h of degradation process, tensile strength of samples with and without IPPD becomes similar (Fig. 4). The differences in mechanical properties become negligible once IPPD disappears of the mass of the samples for a long period of thermo degradation.

The results of elongation at break (Fig. 5) and toughness (Fig. 6) show higher values for the samples containing IPPD until 84 h of exposure. These
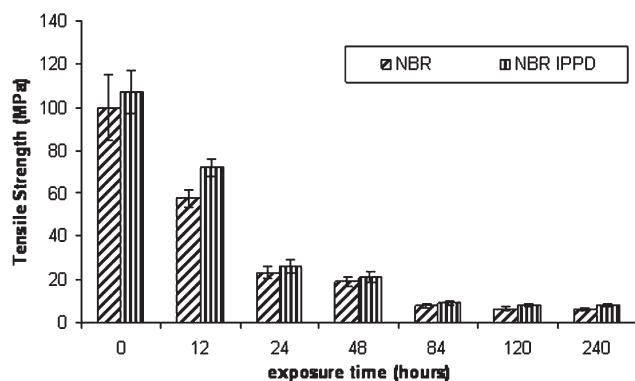
Figure 4 Tensile Strengh of NBR and NBR$_{IPPD}$ exposed to different periods of thermooxidation (0–240 h).

results are consistent with the aforementioned behavior observed for tensile strength. The presence of DOP in the core of the NBR$_{IPPD}$, produces better results of the elongation at break and toughness until 84 h of thermo degradation process. When the effect of IPPD decreases and the DOP disappears, both types of samples show the same evolution.

The evolution of Young's modulus (Fig. 7) and hardness (Fig. 8) in samples with or without IPPD is quite different. Samples containing IPPD show a slower increase in hardness and Young's modulus. The increase in these properties is related to the crosslinking of the samples that appears during the thermo-oxidative treatment.[12]

For short and middle thermo-oxidation exposures (until 48 h) the Young's modulus values remain very low (Fig. 7). The degradation is not enough to produce a high increase in stiffness of the samples. Samples with and without IPPD show similar evolution. At exposure times, above 48 h the values of Young's modulus increase significantly and clear differences between both types of samples appear. The samples without antioxidant have a higher
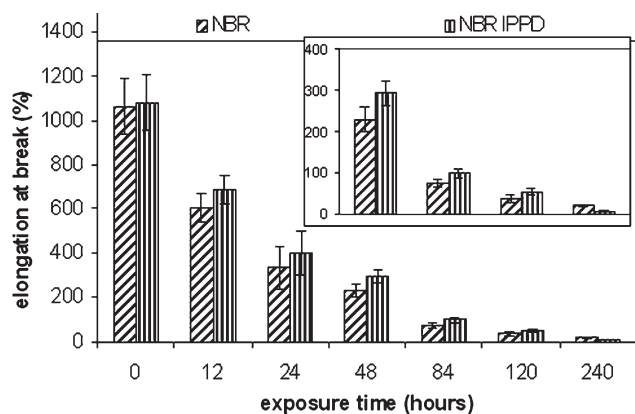

Figure 6 Toughness of NBR and NBR$_{IPPD}$ exposed to different periods of thermooxidation (0–240 h). The inset shows an expanded view of the last stage of the Toughness (48–240 h).

Young's modulus and have lost elasticity. This behavior is attributed to: (i) part of the DOP present in the core of the rubber has been eliminated producing fragilization of the sample and (ii) the presence of IPPD avoids a major crosslinking that would result in an increase in stiffness. The results agree with the decrease in carbonyl groups observed by ATR-FTIR.

Initial values of hardness for samples with and without IPPD are not significantly different. Hardness is a characteristic related to the surface of the sample. As it was expected, samples without IPPD tend to yield higher hardness for long periods of thermo degradation process. IPPD prevents surface crosslinking while there is enough amount of it on the surface. This behavior is consistent with the ATR-FTIR spectra presented (Fig. 2). The bands at 1599 and 1517 cm^{-1}, assigned to IPPD, which are initially present in non exposed NBR$_{IPPD}$, disappear when the samples are submitted to exposure periods longer than 84 h of thermo-oxidation treatment.

Figure 5 Elongation at break of NBR and NBR$_{IPPD}$ exposed to different periods of thermooxidation (0–240 h). The inset shows an expanded view of the last stage of the elongation at break (%) (48–240 h).
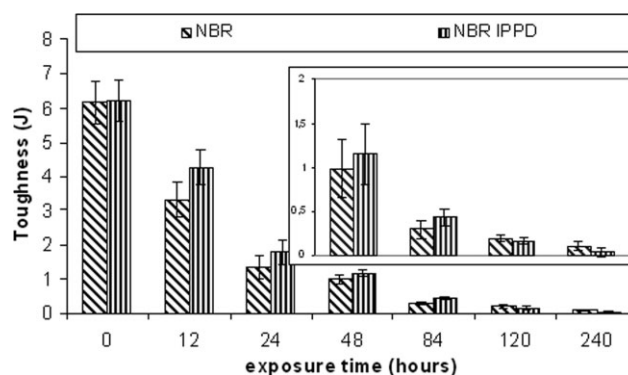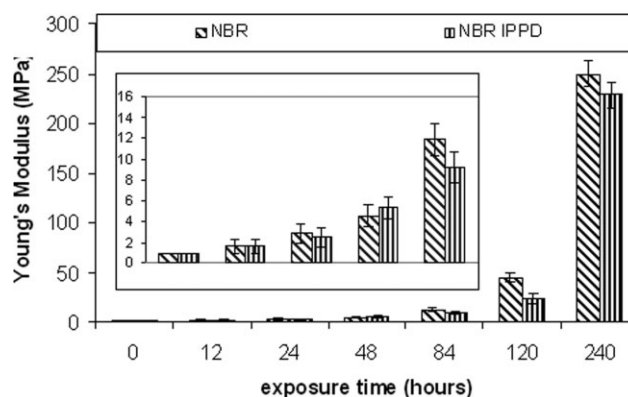

Figure 7 Young's modulus of NBR and NBR$_{IPPD}$ exposed to different periods of thermooxidation (0–240 h). The inset shows an expanded view of the first stage of Young's modulus (MPa) (0–48 h).
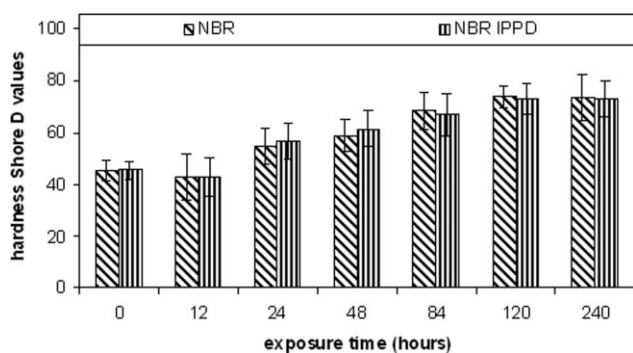
Figure 8 Hardness of NBR and NBR$_{IPPD}$ exposed to different periods of thermooxidation (0–240 h).

After this initial period, the values of hardness of both types of samples are similar.

Crosslinking

The average Molecular mass M_W (g/mol) of the different thermo-oxidized samples is shown in Figure 9. As it was expected, M_W decreases (crosslinking increases) in relation to time of thermo-oxidation treatment. Since the samples contain an important amount of silica the values of M_W between knots are not absolute. The actual values should be higher than those of the graphic. However, the trend and the velocity of crosslinking are believable.

A parallelism between samples with and without IPPD can be observed until 84 h. From 84 to 120 h of exposure, the M_W of NBR decreases drastically (65%) in relation to NBR$_{IPPD}$ (18%). These results are consistent with the evolution of Young's modulus discussed before. Crosslinking develops from the surface to the core, and in NBR samples the crosslinking is higher than in NBR$_{IPPD}$.

SEM

The fracture analysis of the composites subjected to mechanical testing, especially those without IPPD,
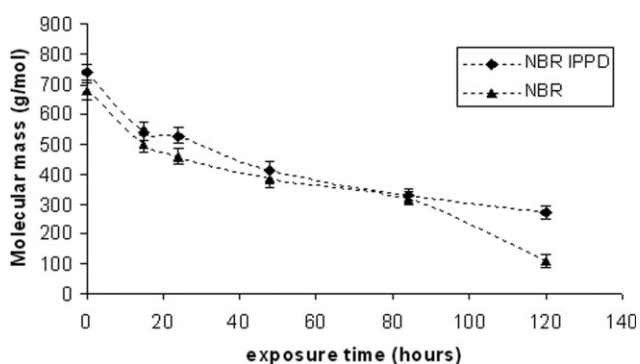

Figure 9 Evolution of crosslink density (M_W) as a function thermo-oxidation exposure time, for each NBR sample.
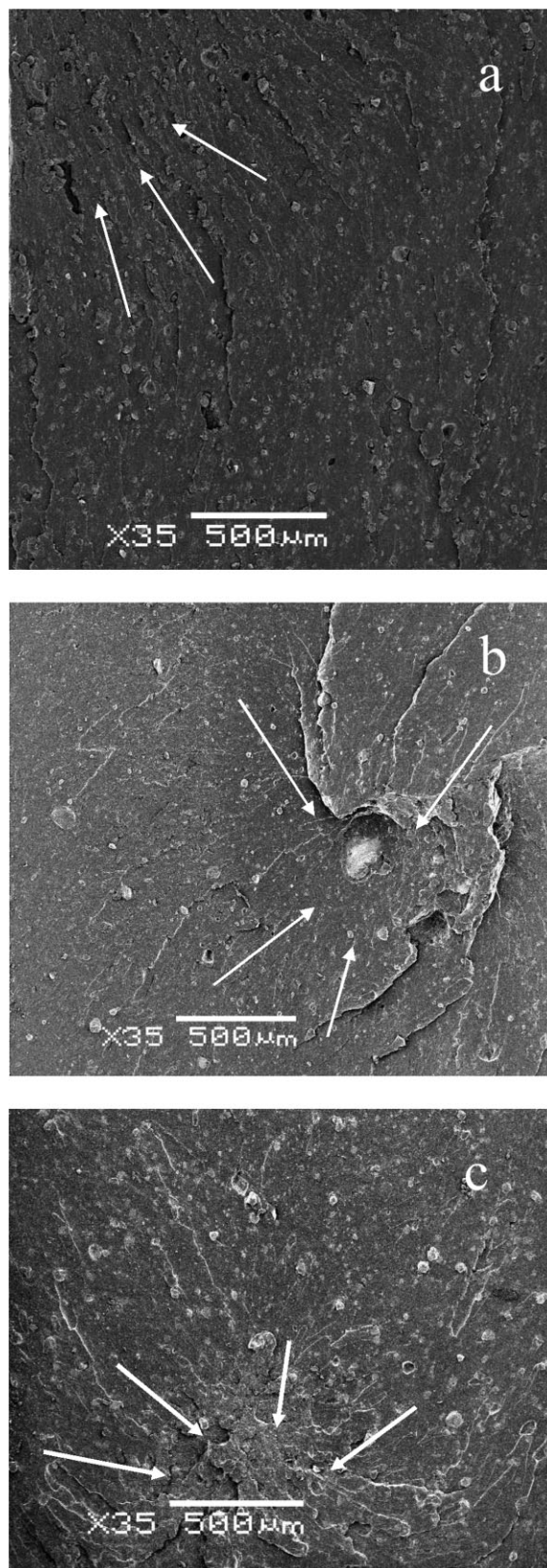

Figure 10 NBR fracture surface (arrows point areas showing matrix deformation): a- without antioxidant at 0 h of exposure time. b- without antioxidant at 84 h of exposure time c- with IPPD antioxidant at 84 h of exposure time.
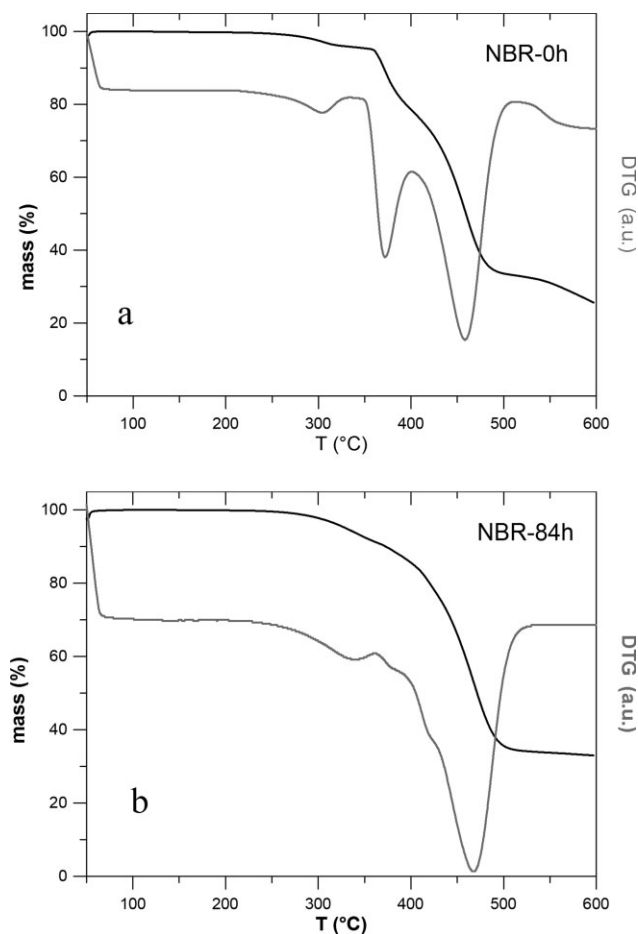
Figure 11 TG scans of NBR as a function of thermo-oxidation exposure: a, −0 h and b, −84 h.

showed a characteristic behavior analogous to exfoliation. The material seemed to break in the form of thin layers. SEM examination was conducted on the fracture section of samples submitted to mechanical testing to investigate the exfoliation of layers as a function of thermal oxidizing time. Figure 10 shows several microphotographies of NBR and NBR$_{IPPD}$ submitted to 0 and 84 h of thermodegradation. The presented microphotographies cover the full area of the section of the test sample, left and right sides of the specimen are coincident with the frame of the photograph, and the center of the superior and inferior border of the frame define the line that would be the symmetry axis of the test piece in the longitudinal sense of the fracture area. The areas where the matrix shows deformation have been pointed with white arrows. The absence of antioxidant yields a more brittle surface. To corroborate this assertion, Figure 10(a) shows a fracture where the matrix deformation is located close to the surface of the specimen. This suggests that the surface is not more brittle than the core of the sample. In this case crosslinking related to degradation is not present. Figure 10(b) corresponding to NBR at 84 h of thermo-

oxidizing shows a fracture located in a defect of interface with a SiO$_2$ particle agglomerate. The rest of the fracture presents exfoliation that leads to a clean fracture surface. On the other hand, Figure 10(c) shows that when IPPD is present, only a mild exfoliation takes place; fracture is less brittle. It is significant that the area where the matrix shows deformation is located in the central area of the test sample (left and right borders are coincident with the sides of the specimen). This distribution suggests a lower crosslinking in the core of the sample than near to the surface. The SEM analysis is in consonance with the improvement of mechanical properties achieved by IPPD antioxidant, mainly tensile strength and Young's modulus.

TG

Figures 11 and 12 show the thermogravimetric (TG) results of analysis of NBR and NBR$_{IPPD}$ samples. The figures show the variation of mass during heat treatment in an air atmosphere. The mass loss can be divided into three stages in all cases, although the absolute values for temperature and the
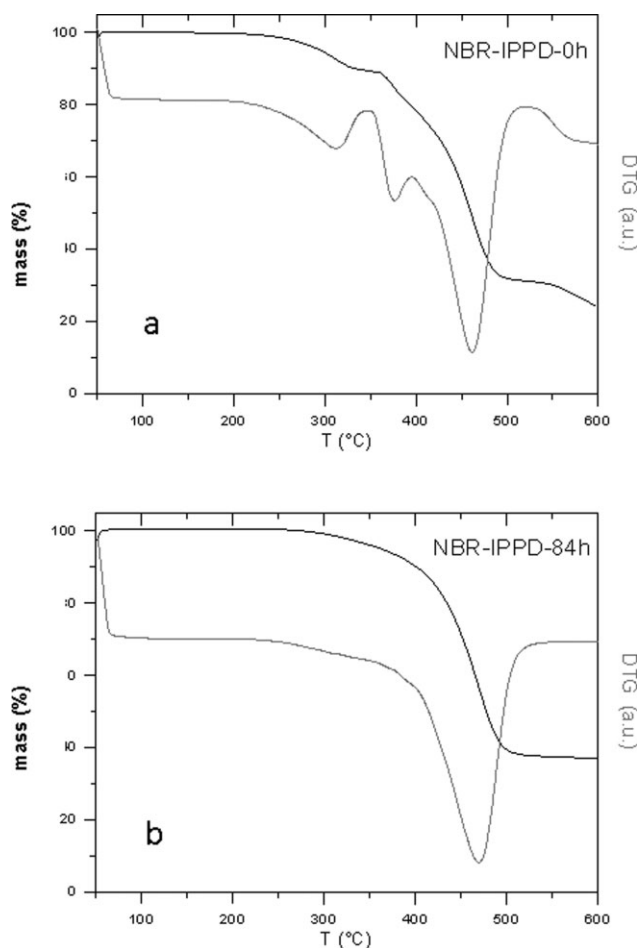

Figure 12 TG scans of NBR$_{IPPD}$ as a function of thermo-oxidation exposure: a, −0 h and b, −84 h.

percentage of mass loss are different for each composite. Figure 11 shows the results of samples without antioxidant. The initial content of DOP in these samples is 17.1%. At 371°C there is a mass loss in samples without previous degradation [Fig. 11(a)] that is related to the decrease in DOP content.[27] To evaluate this decrement we have determined the variation of mass that takes place at this temperature and used as reference the silica content of the samples which remains unaffected at the end of the heating process. By using this estimation, after 84 h of thermo-oxidation treatment the amount of DOP falls to 2% at 383°C [Fig. 11(b)] (a loss of 88,3% during 84 h of thermal exposure). Same procedure applied to NBR$_{IPPD}$ samples shows a DOP mass loss at same temperatures and treatment time of 75% (Fig. 12). Both types of samples with and without IPPD show a second important mass loss at temperatures about 460°C. According to the TG studies by Broska et al.,[28] this phenomenon is associated with the degradation of NBR. Referring the mass variation at this temperature to the final weight of the analyzed sample, the loss of NBR observed during the first 84 h of treatment is 8.2% in case of NBR and 2.1% for NBR$_{IPPD}$. These values allowed concluding that the presence of IPPD reduces the degradation process, at least during the first 84 h of thermo-oxidative treatment. The obtained results are in agreement with the ATR-FTIR, the mechanical properties and the evolution of crosslinking were discussed previously.

CONCLUSIONS

Addition of IPPD antioxidant agent improves the endurance to thermo-oxidation but not for long periods of exposure to thermo-oxidation. After 84 h of treatment a significant decrease in the composite elasticity and tensile strength was observed due to the degradation and disappearance of IPPD agent. Mechanical properties of NBR increase when IPPD is present but samples submitted to long-term treatments show similar behavior with or without antioxidant. The evolution of some groups as carbonyl group, increasing at the beginning of the process and eventually decreasing, or the disappearance of ZnO are indications of the migration processes present during the thermal processes. The band at 1640 cm^{-1}, assigned to unsaturations, increases with thermo-oxidation time. Those double bonds act as crosslinking sites allowing the development of surface stiffness, the composite builds a network. Stiffness increases when plasticizers (DOP) disappear

from the surface. When IPPD is present, a lower degree of crosslinking versus time is observed. This is also observed by ATR-FTIR results that show a slower decrease in methylene and methyl groups of the NBR matrix.

References

1. Al-Malaika, S.; Peng, X. Polym Degrad Stab 2007, 92, 2136.
2. Carrasco, F.; Pagès, P.; Pascual, S.; Colom, X. Eur Polym J 2001, 37, 1457.
3. Colin, X.; Audouin, L.; Verdu, J. Polym Degrad Stab 2007, 92, 906.
4. Dos Santos, K. A. M.; Suarez, P. A. Z.; Rubim, J. C. Polym Degrad Stab 2005, 90, 34.
5. Colom, X.; Andreu, F.; Carrillo, F.; Nogués, F. AFINIDAD 2005, 62, 274.
6. Colom, X.; Andreu, F.; Carrillo, F.; Cañavate, F. AFINIDAD 2008, 65, 25.
7. Polovkova, J.; Kortisova, I.; Gatial, A.; Breza, M. Polym Degrad Stab 2006, 91, 1775.
8. Gatial, A.; Polovkova, J.; Kortisova, I.; Breza, M. Vibrational Spectrosc 2007, 44, 1.
9. Cibulkova, Z.; Simon, P.; Lehocky, P.; Balko, J. Polym Degrad Stab 2005, 87, 479.
10. Klein, E.; Matis, M.; Lukes, V.; Cibulkova, Z. Polym Degrad Stab 2006, 91, 262.
11. Li, G. Y.; Koenig, J. L. Appl Spectrosc 2002, 56, 1390.
12. Li, G. Y.; Koenig, J. L. Polym Degrad Stab 2003, 81, 377.
13. Stenberg, B.; Shur, J.; Jansson, J. F. J Appl Polym Sci Appl Polym Symp 1979, 35, 511.
14. ISO 37:1994 Rubber, Vulcanized or Thermoplastic. Determination of Tensile Stress-Strain Properties.
15. ISO 4577:1983 Determination of thermal oxidative stability in air - Oven method.
16. Flory, J.; Rhener, J. J Chem Phys 1943, 11, 5120.
17. Ellis, B.; Welding, G. W. Rubber Chem Technol 1964, 37, 571.
18. Hildebrand, J. H.; Scott, R. L. The Solution of Non Electrolyte, 3rd ed.; Van Nostrand Reinhold: New York, 1950.
19. Coates, J. Interpretation of Infrared Spectra. A Practical Approach; Meyers, R. A., Eds.; Wiley: New York, 1999.
20. Socrates, G. Infrared and Raman Characteristic Group Frequencies: Tables and Charts; John Wiley & Sons Inc: New York, 2004.
21. Colthup, N. B.; Daly, L. H.; Wiberly, S. E. Introduction to Infrared and Raman Spectroscopy; Academic Press: California, 1990.
22. Mrklic, Z.; Kovacic, T. Thermochim Acta 1998, 322, 129.
23. Delor, F.; Lacoste, J.; Lemaire, J.; Barrois-Odin, N.; Cardine, C. Polym Degrad Stab 1996, 53, 361.
24. Virgilia, L.; Giantomassia, F.; Pugnalonia, A.; Mattioli-Belmontea, M.; Natalia, D.; Tarsib, R.; Contic, C.; Tosic, G.; Marguttad, M.; Bonorae, M.; Biaginia, G. Polym Degrad Stab 2005, 87, 143.
25. Atek, D.; Belhaneche-Bensemra, N. Eur Polym J 2005, 41, 707.
26. Chaudry, A. N.; Billingham, N. C. Polym Degrad Stab 2001, 73, 505.
27. Shieh, Y.; Liu, C. J Appl Polym Sci 2001, 82, 3591.
28. Broska, R.; Billingham, N.; Fearon, P. Polym Degrad Stab 2008, 93, 1100.